Molecular Structure of Surface Active Salt Solutions: Photoelectron Spectroscopy and Molecular Dynamics Simulations of Aqueous Tetrabutyl-ammonium Iodide

Bernd Winter,* Ramona Weber, Philipp M. Schmidt, and Ingolf V. Hertel†
Max Born Institute, Max-Born-Straße 2A, 12489 Berlin, Germany

Manfred Faubel
Max-Planck-Institut für Strömungsforschung, Bunsenstr. 10, 27073 Göttingen

Luboš Vrbka and Pavel Jungwirth‡
Institute of Organic Chemistry and Biochemistry
Academy of Sciences of the Czech Republic and and
Center for Complex Molecular Systems and Biomolecules,
Flemingovo nam. 2, 16610 Prague 6, Czech Republic
(Dated: February 9, 2004)

We report photoelectron measurements and molecular dynamics simulations with a polarizable force field of surface-active aqueous tetrabutyl-ammonium iodide (TBAI). Photoemission was studied for 100 eV photon energy using a 6 μm diameter liquid jet. Surfactant activity of the TBAI salt at the solution surface is documented by a dramatic ($\times$70) increase of the I^-(4d) signal as compared to a NaI aqueous solution for identical salt concentrations. Completion of the segregation monolayer is identified through the growth of both the iodide photoelectron emission signal as a function of the salt concentration. Our experiments reveal identical electron binding energies of iodide in TBAI and NaI aqueous solutions which are independent of the salt concentration. No spectral shifts due to work function changes are observed, hence no dipole is formed by TBA^+ and I^- ion pairs perpendicular to the solution surface. The experimental observations are consistent with results of molecular dynamics simulations of slabs of aqueous TBAI. Both cations and anions are found to exhibit a strong surfactant activity, failing thus to form an electric double-layer. While the cations are surface bound due to hydrophobic interactions, iodide is driven to the vacuum/water interface by its large polarizability. Molecular dynamics simulations also allow characterizing the thermally averaged geometries of the surface-active cations, in particular the orientations of the butyl chains with respect to the water surface.

PACS numbers: 79.60.-i,87.64.Lg

I. INTRODUCTION

Present understanding of hydration of solute ions, and in particular the knowledge about segregation of ion pairs at the water surface, is far from being complete. This is true for both the electrostrictive hydration as in the case of alkali-halide salts [1], and the water structure enforced [2] ion pairing (hydrophobic hydration) as typically encountered for nonpolar organic solutes. The present study is concerned with the molecular structure of the surface region of tetrabutyl-ammonium iodide (TBAI) aqueous solution. TBAI is one of the most efficient and intensively investigated phase-transfer catalysts [3]. In formamide solution depth profiling by photoelectron spectroscopy has revealed that the salt forms a surface monolayer of about 1 nm thickness, roughly corresponding to the size of the TBA^+ cation [4, 5]. Comparable experiments in aqueous solution have so far not been reported as a consequence of the substantially higher vapor pressure of water.

Surface segregation of the TBAI molecule has been ascribed to the formation of ion pairs within the same cavity as this minimizes the total disturbance of the water structure by both the anion and the large hydrophobic cation. In that way a higher surface concentration as compared to non-paired ions may be obtained [4]. The effect scales with the anion size. Generally, little is known about the actual molecular structure of the hydrophobic TBA^+ cation at the solution surface, however several structural models have been proposed for TBAI in formamide [5, 6]. Also, the precise location of the iodide anions is unclear. Is there also a propensity for I^- to reside in the top surface layer or do the TBA^+ and I^- ions rather pair perpendicular to the surface to create an electric double layer? In this context even iodide partial dehydration has been proposed [7].

Photoelectron spectroscopy at appropriate photon energies is reasonably surface-sensitive which makes this technique an attractive tool for unravelling these questions. However, until recently photoemission was hardly applicable to highly volatile liquids due to the difficulty to transfer electrons from the liquid surface through the

*Electronic address: bwinter@mbi-berlin.de
†Corresponding author; Electronic address: hertel@mbi-berlin.de; also at Freie Universität Berlin, Physics Department; URL: http://staff.mbi-berlin.de/hertel
‡Electronic address: pavel.jungwirth@uochb.cas.cz

vapor phase to an electron detector. In the present work photoemission from a liquid microjet is studied by 100 eV photons allowing to probe an information depth of about 2-3 water layers [8]. In addition, this photon energy matches the maximum of the shape resonance in the $I^-(4d)$ photoionization cross section of aqueous iodide which enables the detection of the iodide signal for TBAI concentrations as low as 0.005 m (molal = mol/kg solvent).

Two key aspects are addressed by the present experiments: (i) peak shifts in the photoemission spectra which can correlate with changes in either the electron binding energy or the work function, and (ii) the evolution of the ion signal as a function of the salt concentration.

Molecular dynamics (MD) simulations serve as a valuable tool for interpreting such experiments at the molecular level. In particular, there is a well developed strategy for modelling the extended vacuum/solution interface using periodic boundary condition in the slab geometry [9]. Such simulations allow one to study the distribution of the salt ions when moving from the interface to the aqueous bulk. While small hard atomic ions are repelled from the interface, in accord with the traditional theory of surfaces of electrolytes [10], large molecular ions containing hydrophobic groups exhibit surfactant activity [11]. Very interesting is also the behavior of soft atomic anions such as iodide, which were shown to be driven to the vacuum/water interface primarily due to their large polarizability [12, 13].

In the present study, we perform MD simulations with a polarizable force field of aqueous slabs with varying amounts of TBAI. The principal goal is to provide a molecular interpretation of the experimental results in terms of the distribution of the cations and anions in the bulk solution and, in particular, at the vacuum/water interface. To this end we evaluate thermodynamically averaged density profiles of TBA and iodide ions across the water slab together with the profiles of the resulting charge distributions. At the same time, we are able to characterize the preferred geometries and orientations of the TBA cations at the surface.

The rest of the paper is organized as follows. In Section II we describe in detail the experimental and computational methods. Section III presents and analyzes the results from photoelectron experiments as well as form MD simulations. Finally, a summary is provided in Section IV.

II. EXPERIMENTAL AND COMPUTATIONAL METHODS

A. Experimental

The liquid micron-sized water jet, 6 μm in diameter, is generated in a high-vacuum environment in order to make photoelectron spectroscopy applicable to a highly volatile liquid. This small beam size results in nearly collisionless evaporation [14]. A detailed description of the setup has been given elsewhere [8]. Briefly, the jet, having a temperature of 4°C, is formed by injecting the liquid at 80 bar He pressure through a 10 μm diameter orifice [8, 14]. At the exit of the nozzle the beam contracts to 6 μm [14–16] and acquires a final velocity of about $u = 125\,\mathrm{ms}^{-1}$. Over a distance of $3-5$ mm downstream from the nozzle the beam is laminar having a smooth surface. The working pressure in the main chamber containing the jet is 10^{-5} mbar. Photoelectrons pass through a 100 μm orifice, which separates the main chamber from the electron detection chamber. The latter is equipped with a hemispherical electron energy analyzer (Specs/Leybold EA 10/100) and a single electron multiplier detector for electron counting. Highly demineralized water was used in the experiments and salts were of highest quality commercially available (p.a., Aldrich).

The photoemission measurements were performed at the MBI-BESSY undulator beamline (U125), providing photon energies up to about 180 eV at an energy resolution better than 6000. For the present experiments the resolution was reduced to about 100 meV in favor of the photoelectron emission signal which is more than sufficient to resolve the observed structures with their intrinsic width of typically > 0.5 eV. At a photon flux of about 4×10^{12}/s per 0.1 A ring current count rates on the order of $10-100$ counts per second at peak maximum were obtained. The synchrotron light intersects the laminar liquid jet at normal incidence. Electrons are detected in normal direction to both the jet and the light polarization vector. The count rates in all spectra reported in the present work are normalized to the ring current, so that the intensities for different species or concentrations within one graph can be directly compared to each other.

B. Molecular dynamics simulations

Molecular dynamics (MD) simulations were carried out using the AMBER7 software package [17] with polarizable potentials [18, 19]. We used the parm99.dat force field [20] with a slight modification of the iodide anion polarizability [19]. A water slab consisting of 863 POL3 water molecules [21] was used for the construction of the following two systems. The first system contained in addition a single TBAI ion pair with the cation and anion initially located on the same side of the aqueous slab (corresponding to a concentration of ~ 0.06 m). The second system contained initially 8 TBAI ion pairs on each side of the water slab, i.e. 16 TBAI pairs in total (~ 1 m). Both systems were placed in rectangular boxes with dimensions of $31\times31\times100\,\text{Å}^3$. Periodic boundary conditions were applied in all three dimensions to produce an infinite water slab in the $xy-$ plane with two air-water interfaces perpendicular to the $z-$ direction. A 12 Å cutoff distance was applied to the van der Waals and electrostatic interactions. The particle mesh Ewald procedure [22] was used to account for the long range electrostatic

interactions. All bonds including hydrogen atoms were constrained using the SHAKE algorithm [23].

In the beginning, 15 000 steps of steepest descent minimization were performed for all systems to remove bad contacts potentially introduced during the build up phase. After minimizations, simulations started at 10 K. Temperature was gradually increased to 300 K during a 50 ps heating period, after which a 500 ps equilibration followed. Finally, data were gathered during a 1 ns production run. Coordinates and induced dipoles were monitored every 500 steps. A time step of 1 fs was used for the integration of the equations of motion. All the MD simulations were performed in the canonical ensemble (NVT) with temperature held fixed at 300 K (except for the initial heating period) using the Berendsen temperature coupling scheme[24].

All trajectories were analyzed to provide density profiles (translational order profiles) for water oxygens, nitrogens of the TBA cations, and iodides, charge distribution profiles and induced dipole profiles. For obtaining these profiles, the simulation box was divided into 0.2 Å slices perpendicular to the $z-$coordinate. Preferred orientations of the TBA cation butyl chains were also investigated. To this end angles between the normal to the surface where the cation resided and vectors defined by the cation nitrogen and the terminal butyl carbon atoms were monitored.

III. RESULTS AND DISCUSSION

A. Photoemission Measurements

In Figure 1 typical photoemission spectra obtained for 100 eV photon energy from the pure water solvent, of a 0.025 m TBAI aqueous solution and, for comparison, of a 2 m NaI aqueous solution are presented. The spectra are vertically displaced with respect to each other. Relative intensities are scaled to the synchrotron beam current, i.e. to the photon flux. The decreasing water feature intensity, from bottom to top, reflects the attenuation of the water signal for the respective salt solutions. The energy axis refers to electron binding energies with respect to vacuum [1, 8].

The photoemission spectrum of pure liquid water (bottom) arises from the H_2O molecular orbitals $1b_1$, $3a_1$, $1b_2$, and $2a_1$. In addition it shows the characteristic energy losses experienced by low-kinetic electrons travelling through the liquid [8]. The extra features in the NaI-aqueous solution (middle) arise from Na^+ and I^- as assigned and discussed in detail elsewhere [1]. In the TBAI spectrum (top) the prominent iodide doublet, $I^-(4d)$ at $53.8 - 55.3$ eV, is found to be almost as intense as for the NaI solution even though the concentration of the former solution is 80 times lower. This documents in a very direct manner substantial surface segregation. Note that there is only a small contribution from TBA^+ to the photoelectron spectrum; the only noticeable peak

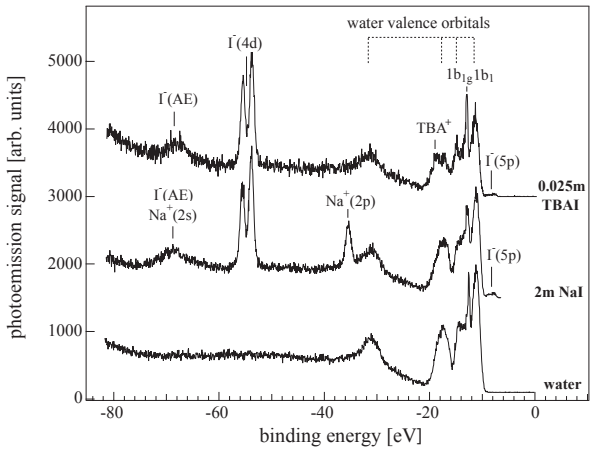

FIG. 1: Photoemission spectra of pure water (bottom), 2 m NaI (middle), and 0.025 m TBAI aqueous solutions (top) obtained for 100 eV photon energy. The emission from ions is labelled. Electron binding energies are with respect to vacuum. Intensities are normalized with respect to the ring current. Measured $I^-(4d)$ intensities are almost identical even though the concentrations differ by a factor of 80.

arising near 19 eV strongly overlaps with the water features. Clearly, for charge neutrality there must be equal amounts of anions and cations at the surface. With the $I^-(4d)$ iodide signal ratio $I^-(TBAI)/I^-(NaI)$ being 0.9, as inferred from Figure 1, and the corresponding iodide concentration ratio of 1/80, the effective segregation factor for the given concentrations is about 70.

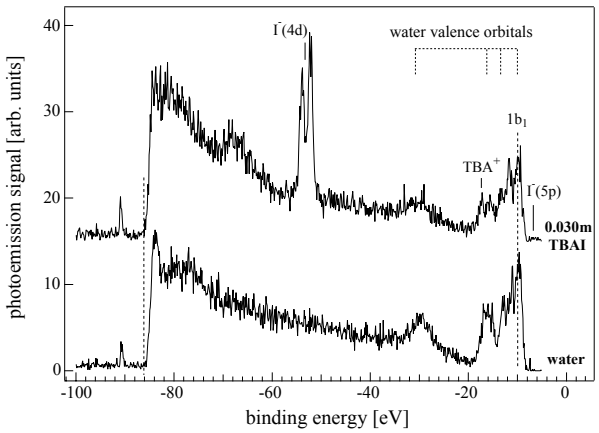

FIG. 2: Comparison of the full-range photoelectron emission spectra from pure liquid water vs. 0.030 m TBAI aqueous solution obtained for 100 eV photon energy. Identical peak positions are observed for the cutoff regions and for the water valence features as indicated by the vertical lines.

A comparison of the cutoff region of the spectra for pure water vs. a TBAI solution might help to identify

the existence of surface dipoles (orientated ion pairs) with a component normal to the solution surface. In Figure 2 we show full-range photoemission spectra of a pure water spectrum and of a 0.03m TBAI (ca. 33% of saturation concentration) spectrum. Again, the photon energy was 100 eV. Both spectra exhibit very similar cutoffs, with no evidence for energy shifts. We also note that the water features appear at identical peak positions for the two solutions. These findings are consistent with a surface structure in which both anions and cations are located within the top surface layer. Hence, also the iodide shows surfactant activity arising from its large polarizability as will be detailed below. We emphasize that these results are not consistent with the formation of an electric double layer at the surface [3].

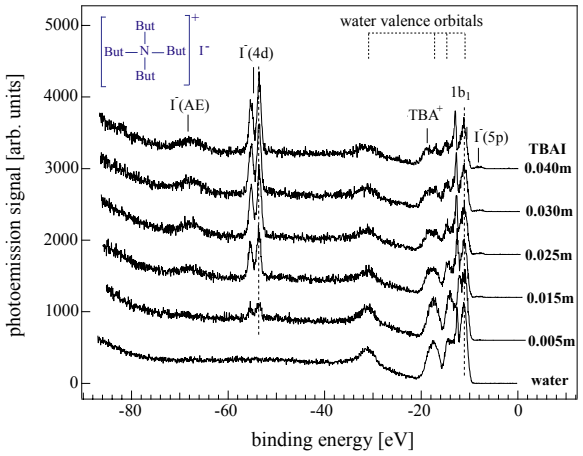

FIG. 3: Photoelectron spectra of TBAI aqueous solutions for different salt concentrations, as labelled. The photon energy used for photoemission was 100 eV. Intensities in the spectra are normalized to the synchrotron photon flux.

More detailed information on the molecular structure at the surface of the TBAI solution may be obtained by studying the photoelectron signal as a function of the salt concentration. Selected photoemission spectra for different concentrations of TBAI in water, are displayed in Figure 3 along with a reference spectrum of pure water. The relative intensity changes directly reflect the water signal attenuation as the overlayer evolves. No differential peak shifts are observable as illustrated by the vertical lines. The fact that iodide electron binding energies are constant (within ±30 meV) [1] over the entire range of TBAI concentrations investigated is not consistent with the observed decrease of the threshold energy for photoionization of solvated iodide for increasing salt concentration reported previously [7]. One may argue, that this discrepancy arises from some spectral shift (possibly due to charging) in the previous experiment, which for threshold experiments may be difficult to identify in the absence of a well-defined reference energy. Hence, our results do not support the reported decrease of ionization potential of aqueous iodide in the presence of surface active cations, which has been interpreted in terms of a (partial) dehydration effect [7]. In fact, previous combined MD and ab initio calculations of iodide in/on a water slab showed, that the ionization potential practically does not change upon moving the anion from the bulk to the aqueous surface [25]. This is due to the fact that a partial loss of the solvation shell is more than compensated at the surface by polarization interactions [12].

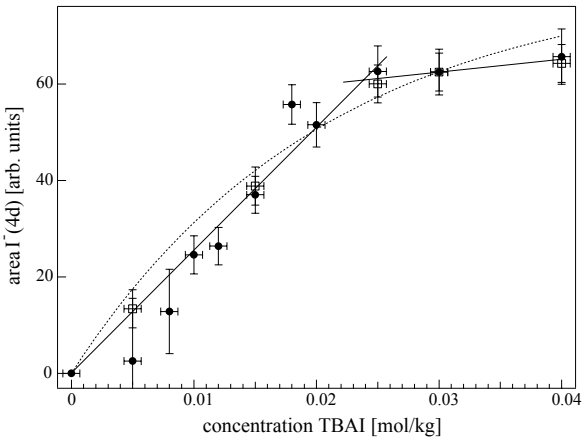

FIG. 4: Evolution of the I^-(4d) photoelectron emission signal as a function of the TBAI concentration c. Circles are derived from the measurements shown in Fig. 3, and squares result from another set of measurements. The dotted curve is a fit $\propto [1 - \exp(c/c_0)]$. The straight (full) lines indicate a linear growth of a single monolayer reflecting the successive completion of the surface segregation layer near 0.02 m.

The quantitative analysis of the iodide photoemission signal as a function of the TBAI concentration is displayed in Figure 4. Each data point represents the integral of the I^-(4d) emission feature, derived from the data by assuming Gaussian line shapes with a constant background. Indicated errors are statistical errors. An additional set of data points from a different series of measurements (full circles) improves the statistics. Unfortunately, due to strong peak overlap we were not able to extract quantitatively the corresponding plot for attenuation of the water signal but the general behavior of the water signal confirms the trend observed for I^-(4d) attenuation.

Qualitatively two regimes can be distinguished in Figure 4. For concentrations smaller than about 0.024 m the iodide signal rises about linearly with increasing concentration, which may be identified as the regime of sub-monolayer coverage. The much slower intensity increase for concentrations beyond 0.024 m would then reflect the completed segregation monolayer. Two linear lines (dashed) have been drawn to guide the eye. The full line in Figure 4 is a fit $\propto [1 - \exp(-c/c_0)]$ which is commonly used to model layer by layer film growth

[26]. It describes the envelope of consecutive linear segments, reflecting the sequential monolayer built-up. The fit parameter $c_o = 0.21$ gives the salt concentration for saturation in the layer by layer model. Obviously such a fit is not convincing which we take as strong evidence for only one monolayer being formed. Then, no contribution from a second an subsequent layer is expected and the experimentally observed signal increases slower the layer by layer fit function. Hence, the break at about 0.024 m concentration marks the completed monolayer. The reason for the continuous, albeit small further increase of the photoelectron signal above 0.024 m is attributed to the filling of remaining cavities within the surface layer as well as to the increase of bulk ion concentration. To understand the thus experimentally derived concentration for monolayer formation we have to recall how the surfaces is formed: it is created only after the jet emerges from the nozzle, and the interaction region with the photon is about $\ell = 4$ mm downstream from the nozzle. Hence, in the beam travelling with a velocity $u = 125\,\mathrm{m\,s^{-1}}$ there is only a time $t = \ell/u \simeq 3 \times 10^{-5}$ s to establish the surface structure. We roughly estimate the number of molecules which could possibly reach the surface during this time, assuming the TBAI molecules to be homogeneously distributed at the orifice. According to Ficks law of diffusion [27] the mean distance L over which an ion travels through a liquid medium during the time t is given by $L = \sqrt{4Dt}$, with $D = 0.52 \times 10^{-5}\,\mathrm{cm^2 s^{-1}}$ being the diffusion constant [28]. One obtains a mean diffusion length of $L \simeq 250$ nm (corresponding to about 800 monolayers of water). At the concentration of saturation $\simeq 0.024$ m we have about 3.6×10^{14} TBAI-molecules in a volume of $1\,\mathrm{cm^2} \times L$. If we assume that in the diffusion process about 1/6 of these molecules have a chance to reach the surface our experimental result would correspond, in this very rough estimate, to a saturation density of 0.6×10^{14} molecules/cm^2. This is in sufficiently good agreement with the theoretical findings (see next section) and in keeping with previous predictions. For comparison we note that a surface completely filled with TBAI molecules would contain about 1.6×10^{14} molecules/ cm^2 (the specific mass of TBAI being $1.2\,\mathrm{g\,cm^{-3}}$, its molecular weight 369.4).

B. MD Results

A first qualitative picture of the surface behavior of TBAI can be obtained from snapshots from the simulations of one of the two vacuum/air interfaces of the slab. Figure 5 shows such typical snapshots displaying the surface coverage of the water slabs with one or 16 TBAI ion pairs, respectively. Note that both TBA^+ cations and iodide anions are present at the surface. The numerical values of the surface coverage for the two systems are $0.1 \times 10^{13}\,\mathrm{cm^{-2}}$and $0.9 \times 10^{14}\,\mathrm{cm^{-2}}$, respectively. This compares very well with the experimental result given in the previous section and a corresponding experimental value predicted for the complete TBAI monolayer is $1.0 \times 10^{14}\,\mathrm{cm^{-2}}$[4]. We recall, that the system with 16 ion pairs corresponds to a concentration about 1 m = 1 mol/kg solvent - an extremely high concentration which can only be reached close to the surface by the surface segregation mechanism. As can be seen from Figure 5 (right) it is unlikely that any additional cation would fit on the surface even though the surface is not completely covered with cations, since the remaining free space is occupied by iodide anions. Density profiles for oxygen, nitrogen and iodide atoms for the systems with a single or 16 TBAI ion pairs are presented in Figure 6.

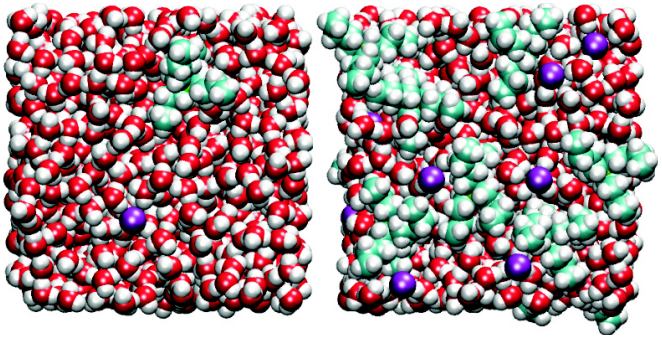

FIG. 5: Snapshots from MD simulations showing the TBAI surface coverage for an aqueous slab containing (left) one, and (right) 16 TBAI ion pairs.

The interfacial region for the latter system is dominated by the high concentration of ions, leading to a decrease of the density of water oxygens. In all simulations both cations and anions clearly prefer positions at the surface. For the cations this behavior is not surprising since TBA^+ is a very well known surfactant. The propensity of the iodide anions for the surface was reported before and was attributed to the effects of polarizability [12, 13, 29]. This is confirmed by our test simulations which show that iodide anions immediately disappear from the surface and prefer full solvation inside the bulk phase when switching off the polarizability part of the force field. Note that the cations remain at the interface even for the non-polarizable force field, since the surface driving force here is the hydrophobic interaction between the butyl groups and water.

In agreement with the present experimental results there is virtually no ion segregation perpendicular to the surface, i.e. both cations and anions share the space of the interfacial layers of the water slab. This is illustrated in Figure 6. The non-zero signal from the cation inside the aqueous bulk for the more concentrated system (see Figure 6, bottom) confirms the completion of the surface monolayer. Indeed, since there is no space left at the surface, and surfactants do not tend to form more than one layer, one particular cation immerses into the bulk and travels there almost freely, accompanied by charge compensating iodide.

The charge density profiles for the two systems un-

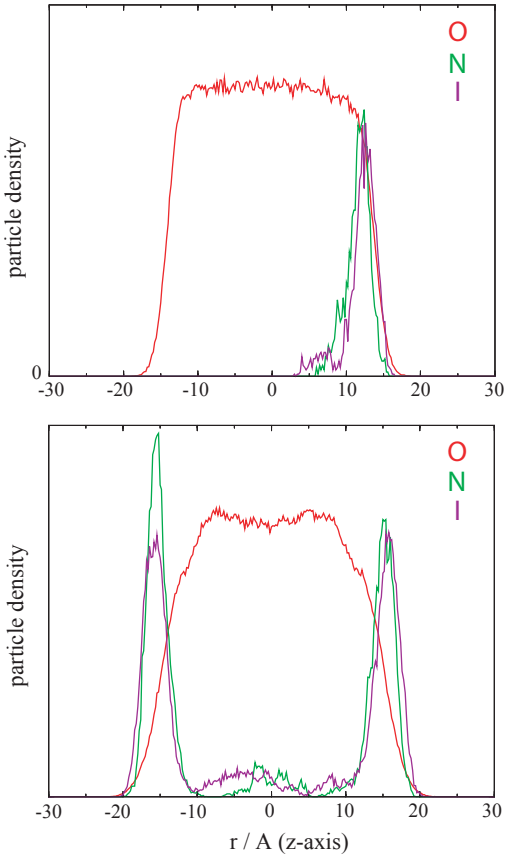

FIG. 6: Snapshots from MD simulations showing the TBAI surface coverage for an aqueous slab containing one (top), and 16 (bottom) TBAI ion pairs.

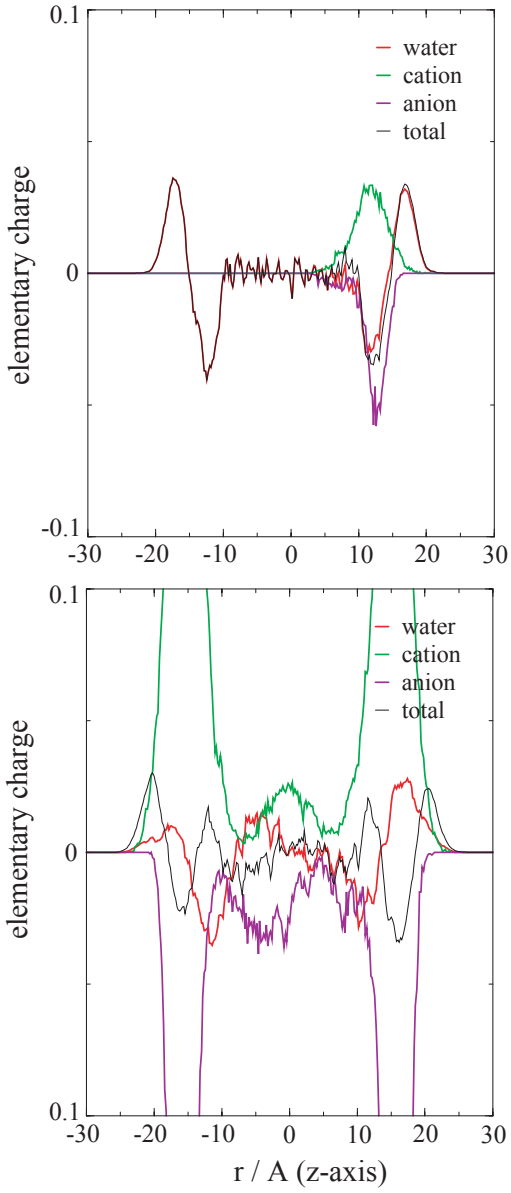

FIG. 7: Charge distribution profiles for one (top), and 16 (bottom) TBAI ion pairs in an aqueous slab.

der study are displayed in Figs. 7. First, we emphasize that the charge variations are in fact rather small, on the order of (or smaller than) $0.1e_0$. Note, for example, that the oxygen atom in the POL3 water model used has a partial charge of $-0.73e_0$. This means we see an excess/depletion of less than 10 % of an oxygen partial charge per volume of $0.2\,\mathrm{nm}^3$. However, the observed non-uniformities in the charge distributions are systematic and well above the statistical noise.

The total charge distributions for the two systems are very similar to each other and exhibit the same basic behavior as that of a neat water slab (not shown here). This is due to the large degree of charge cancellation between the cations and anions, which reside in the same interfacial layer. Moving along the $z-$direction from the surface into the water slab, there is first a region of positive charge ($+0.5e_0$ per surface area of $9.6\,\mathrm{nm}^2$) right at the surface. Then a region of negative charge of the same magnitude follows. The two peaks are separated by approximately 0.5 nm, resulting in a $0.06\,\mathrm{D\ nm}^{-2}$ permanent dipole density at the surface, pointing in the $z-$direction from the slab.

The non-uniformity in the charge distribution is caused by several factors. For the system with a single TBAI ion pair the charge cancellation between the cation and anion is almost perfect (see Figure 7, top). Thus, the observed surface charge distribution arises entirely from the water orientation at the surface, with the positive surface region being due to the dangling hydrogens and the negative region below due to oxygen atoms. The net charge in the bulk, where the water orientation is completely random, is zero.

The situation is more complicated for the system with 16 TBAI ion pairs, where the charge density is much larger. The charge densities of cations and anions still very efficiently cancel each other, however, the remaining charge is non-negligible. Due to the high surface density

of hydrophobic cations there is a reduced amount of water molecules at the interface. This leads to a situation where mainly TBA cations contribute to the positive charge of the interfacial region (see Figure 7, bottom). Moreover, as one of the cations stayed during the simulation inside the bulk phase, accompanied by one or two iodide anions, there are non-systematic charge fluctuation also in the bulk region.

The induced dipoles, present due to the use of a polarizable force field, were also monitored and analyzed. Almost a zero net electric field arising from the random orientation of water molecules causes the induced dipoles inside the water slab to be negligible. For the systems with a single TBAI ion pair, there are two distinct surfaces. The surface without ions exhibits an induced dipole of approximately 0.25 D, which is the same as that observed in our test neat water simulations. The two ions present at the other interface cause an increase of the induced dipole to 1 D. For the system with 16 TBAI ion pairs, the induced dipole at each surface is approximately 2 D. The iodide and water induced dipoles are pointing away from the slab, while the induced dipoles of the cations have the opposite orientation, decreasing thus the total induced dipole at the interface.

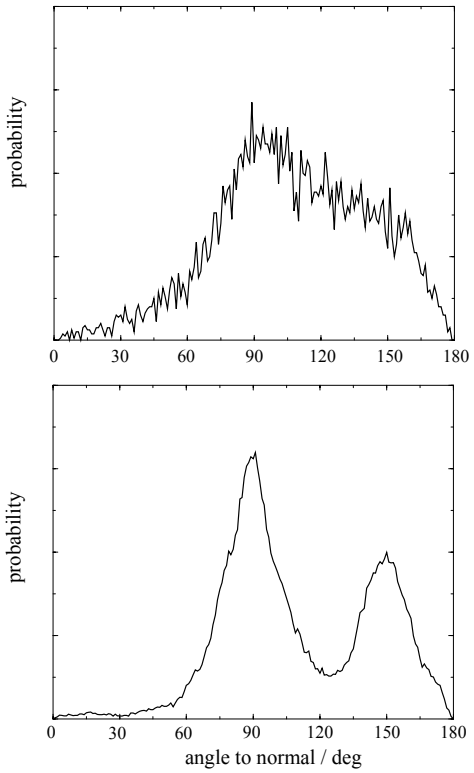

FIG. 8: TBAI butyl chains orientation profiles for one (top), and 16 (bottom) TBAI ion pairs in an aqueous slab.

Unlike iodide, TBA^+ is a complex molecular ion with a flexible internal structure. Orientation profiles of the butyl chains of the TBA cation with respect to the normal to the surface are depicted in Figure 8. The system with a single TBAI ion pair (see Figure 8, top) exhibits only one broad peak for angles between 75^o and 150^o. This means that the butyl chains almost never point into the vacuum but are oriented primarily along the water surface with a slight tendency to point inside the water slab. The situation changes quantitatively for the system with 16 TBAI ion pairs, where two distinct peaks occur, at 90^o and 150^o. The decrease of the population of angles around 120^o for the more concentrated system can be explained by the lack of space at the interface confining the butyl chains to more definite orientations. These results support the previously suggested geometry arrangements of TBA^+ cations at the aqueous surface [5].

IV. SUMMARY

The structure of aqueous tetrabutyl-ammonium iodide at the vacuum/water interface has been investigated by photoelectron spectroscopy and molecular dynamics simulations. The surface sensitive experiment allows to monitor the completion of the segregation monolayer at the surface by the change of the iodide photoemission signal with salt concentration. The experiments also show that the electron binding energies in iodide are independent of the concentration and chemical composition of the counter ions. No spectral shifts due to changes in the work function were observed, hence we conclude that the salt ions do not form an electric double-layer at the surface. The experimental observations are strongly supported by results of molecular dynamics simulations for two different concentrations of TBAI in aqueous slabs using a polarizable force field. The simulations allow for a detailed interpretation of the experiments on a molecular level. In particular, the simulated density profiles clearly show the strong surface propensities of both the hydrophobic TBA cations and the highly polarizable iodide anions. The corresponding charge profiles confirm the non-existence of any appreciable charge segregation perpendicular to the interface. The analysis of the geometries of the flexible TBA cations shows a preference of the orientations of the butyl chains parallel to the surface and, particularly at higher salt concentrations, also towards the aqueous bulk.

Acknowledgments

Support from the Czech Ministry of Education via a grant No. LN00A032 is gratefully acknowledged. We would like to acknowledge C. Pettenkofer and W. Widdra for stimulating discussions. We thank the Supercomputer Center in Brno for a generous allocation of computer time.

[1] Weber, R. *et al. J. Phys. Chem. B* **2003,** in press.
[2] Diamond, R. M. *J. Chem. Phys.* **1963,** *67,* 2513.
[3] Moberg, R.; Bökman, F.; Bohman, O.; Siegbahn, H. *J. Am. Chem. Soc.* **1991,** *113,* 3663.
[4] Holmberg, S.; Moberg, R.; Yuan, Z. C.; Siegbahn, H. *J. Electron Spectrosc.* **1988,** *47,* 27.
[5] Eschen, F.; Heyerhoff, M.; Morgner, H.; Vogt, J. *J. Phys.: Condens. Matter* **1995,** *7,* 1961-1978.
[6] Holmberg, S.; Moberg, R.; Yuan, Z. C.; Siegbahn, H. *J. Electron Spectrosc.* **1986,** *41,* 337.
[7] Watanabe, I.; Takahashi, N.; Tanida, H. *Chem. Phys. Lett.* **1998,** *287,* 714.
[8] Winter, B. *et al. J. Phys. Chem. B* **2004,** in press.
[9] Wilson, M. A.; Pohorille, A. *J. Chem. Phys.* **1991,** *95,* 6005.
[10] Onsager, L.; Samaras, N. N. T. *Chem. Phys.* **1934,** *2,* 528.
[11] Tamaki, K. *Bull. Chem. Soc. Jpn.* **1974,** *47,* 2764.
[12] Jungwirth, P.; Tobias, D. J. *J. Phys. Chem. B* **2001,** *105,* 10468.
[13] Dang, L. X.; Chang, T. M. *J. Phys. Chem. B* **2002,** *106,* 235.
[14] Faubel, M.; Kisters, T. *Nature* **1989,** *339,* 527.
[15] Faubel, M. Photo electron spectroscopy at liquid surfaces. In *Photoionization and Photodetachment*, Vol. 10A; Ng, C. Y., Ed.; World Scientific Publ. Co.: Tokyo, 2000.
[16] Faubel, M.; Steiner, B.; Toennies, J. P. *J. Chem. Phys.* **1997,** *106,* 9013.
[17] Case, D. A. *et al.* "AMBER 7", 2002.
[18] Perera, L.; Berkowitz, M. L. *J. Chem. Phys.* **1994,** *100,* 3085.
[19] Markovich, G.; Perera, L.; Berkowitz, M. L.; Cheshnovsky, O. *J. Chem. Phys.* **1996,** *105,* 2675.
[20] Wang, J.; Cieplak, P.; Kollman, P. A. *J. Comput. Chem.* **2000,** *21,* 1049.
[21] Caldwell, J. W.; Kollman, P. A. *J. Chem. Phys.* **1995,** *99,* 6208.
[22] Essmann, U. *et al. J. Chem. Phys.* **1995,** *103,* 8577.
[23] Ryckaert, J.-P.; Ciccotti, G.; Berendsen, H. J. *J. Comp. Phys.* **1977,** *23,* 327.
[24] Berendsen, H. J. C. *et al. J. Comp. Phys.* **1984,** *81,* 3684.
[25] Bradforth, S. E.; Jungwirth, P. *J. Phys. Chem. A* **2002,** *106,* 1286.
[26] Starr, D. E. *et al. Phys. Rev. Lett.* **2001,** *87,* 106102.
[27] Adamson, A. W. Physical Chemistry of Surfaces John Wiley and Sons, Inc: 1990.
[28] Lide, D. R. *Handbook of Chemistry and Physics;* CRC Press: 1997-1998.
[29] Markovich, G.; Pollack, S.; Giniger, R.; Cheshnovsky, O. *J. Chem. Phys.* **1994,** *101,* 9344.